ChemComm

COMMUNICATION

View Article Online
View Journal

Cite this: DOI: 10.1039/d3cc00475a

Received 2nd February 2023,
Accepted 6th April 2023

DOI: 10.1039/d3cc00475a

rsc.li/chemcomm

Guanidine-based biomimetic hydrides for carbon dioxide reduction†

Junbo Chen, [ab] Haibo Yu, [ab] Davin Tan *[cd] and Richmond Lee *[ab]

The feasibility of various bespoke guanidine-based compounds as biomimetic hydrides were assessed by Density Functional Theory (DFT). The results predicted that tricyclic pentanidine hydrides are viable candidates to reduce CO_2 to $HCOO^-$ and be regenerated electrochemically, demonstrating a recyclable and sustainable method to achieve metal-free electrochemical reduction of CO_2.

One of the main carbon capture storage and utilization (CCSU) strategies to reduce atmospheric CO_2 and mitigate climate change is the direct sequestration and use of CO_2 as a chemical feedstock to create high-value products.[1] The most direct reaction is the molecular reduction of gaseous CO_2 into liquid formic acid or formates ($HCOO^-$) which can be achieved using molecular H_2,[2,3] and hydrides (H^-) such as metal-hydrides,[4] or organo-hydrides.[5] The use of transition metal-based hydrides is also not ideal due to their inherent toxicity and general inavailability.[6] While metallic heterogeneous catalysts are reactive and highly capable of transforming CO_2, a variety of products can be formed and selectivity could be an issue.[7,8] Metal-free organohydrides such as organo-boranes and organo-silanes are also promising, but the main issue is that they are generally employed as single-use sacrificial reagents and lack ease in regenerating the reduced hydride in a circular manner. To this end, biomimetic hydrides might be a better option.

By mimicking the reduced nicotinamide adenine dinucleotide (NADH), nicotinamide adenine dinucleotide phosphate (NADPH) and flavin adenine dinucleotide (FADH) systems in the citric acid cycle during photosynthesis,[9] biomimetic hydrides such as Hantzsch esters[10,11] can act as transfer hydrogenation reagents to efficiently reduce C═C, C═N and C═O bonds in a circular manner (Scheme 1 top) by regenerating the oxidized pyridine back to the Hantzsch ester using H_2[12] or by proton-coupled electron transfer (PCET) process.[13]

Recently, the groups of Glusac,[14,15] Musgraves[16,17] and Ostojić,[18] explored the use of benzimidazoles and diazaphospholenes as biomimetic hydrides to reduce CO_2 through computational and experimental studies (Scheme 1 middle). These systems are NADH analogues, whose reactivity are largely based on the amidine or amidine-like moiety. Inspired by these works, we wanted to explore if guanidine or guanidinium[19–22]

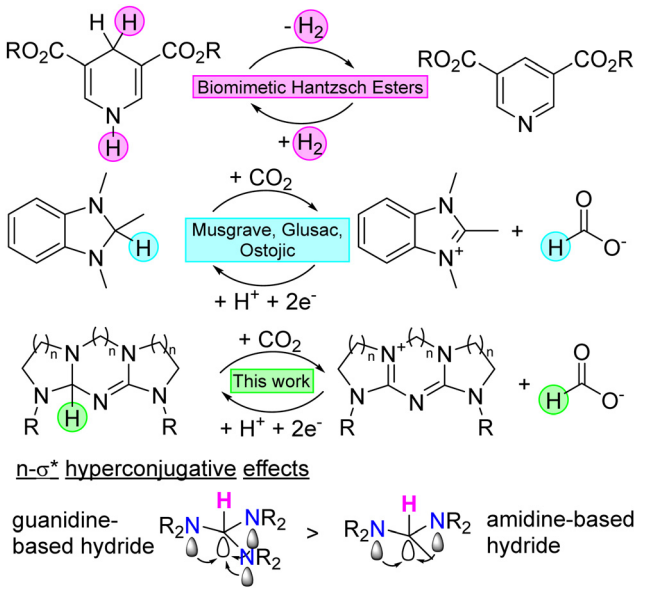

Scheme 1 Biomimetic hydrides such as the commonly used Hantzsch esters, benzimidazole and pentanidine systems. R = alkyl group. Below: n–σ* hyperconjugative effects for amindine- and guanidine-based organohyrdrides.

[a] School of Chemistry and Molecular Bioscience, University of Wollongong, Wollongong, NSW, 2522, Australia. E-mail: richmond_lee@uow.edu.au
[b] Molecular Horizons, University of Wollongong, Wollongong, NSW, 2522, Australia
[c] Institute of Materials Research and Engineering, Agency for Science, Technology and Research, 2 Fusionopolis Way, 138634, Singapore. E-mail: davin_tan@imre.a-star.edu.sg
[d] Institute of Sustainability for Chemicals, Energy and Environment, Agency for Science, Technology and Research, 1 Pesek Road, Jurong Island, 627833, Singapore

† Electronic supplementary information (ESI) available. See DOI: https://doi.org/10.1039/d3cc00475a

can perform as efficiently as Hantzsch esters or biomimetic hydrides (Scheme 1 bottom). Guanidines are well known superbases used in many organic transformations and importantly in this context were investigated to activate CO_2 by forming guanidine–CO_2 adduct,[23,24] but less known is the fact that the central carbon of the Y-shaped CN_3 moiety of guanidinium cations is highly electrophilic and is a suitable hydride acceptor used as n-type dopant in thermoelectrics.[25] Herein, we report a density functional theory (DFT) study to interrogate the feasibility of guanidine-based compounds (guanidines and pentanidines) as organic biomimetic hydrides for CO_2 reduction and this has not been reported to the best of our knowledge. The DFT model predicts a kinetically accessible and thermodynamically favourable metal-free pathway to obtain value-added HCO_2^- from CO_2, whereby the guanidine-based hydrides can be regenerated electrochemically from the guanidinium cations *via* a stepwise $e^- + H^+ + e^-$ pathway, demonstrating a sustainable and carbon-neutral strategy for energy and chemical applications.

A series of acylic, mono-cyclic, bi-cylic and tri-cyclic guanidine-based hydrides were first modelled using DFT with a benchmarked functional and the computational data were focussed on two aspects: the extrapolated Gibbs energy of thermodynamic hydricity, ΔG_{H^-}, for $YH \rightleftharpoons Y^+ + H^-$ (see ESI† Scheme S1 for derivation) and the Gibbs energy barrier for the CO_2 reduction to formate by the organohydride ($\Delta G^{\ddagger}_{CO_2}$). These values for the screened organohydrides are summarized in Table 1. Initial calculations involved modelling the previously studied benzimidazole system (**1a**) using the ωB97XD/6-31+G(d,p)/CPCM(MeCN) level of theory. The calculated ΔG_{H^-} for **1a** is 41.3 kcal mol^{-1} and its $\Delta G^{\ddagger}_{CO_2}$ is 26.5 kcal mol^{-1}. Since **1a** was reported to work experimentally, the energy parameters obtained from computational screening of guanidine hydrides will be compared, and energy values calculated to be lower than that of **1a** would be a good guide to establish any potentially viable biomimetic hydrides. We also modelled two additional imidazolic hydrides that can be achieved synthetically, namely **1b** and **1c**, to investigate whether any variation in the 2-position of the imidazole moiety would affect its ΔG_{H^-} or $\Delta G^{\ddagger}_{CO_2}$. Truncating the methyl group to H (**1b**) or substituting it to a larger phenyl group (**1c**) gave higher ΔG_{H^-} and $\Delta G^{\ddagger}_{CO_2}$. The calculations now focussed on a series of guanidine-based hydrides which theoretically would have better ΔG_{H^-} and $\Delta G^{\ddagger}_{CO_2}$ due to negative hyperconjugation of the three N lone pairs into the anti-bonding orbital of the C–H bond (Scheme 1).[26,27]

The first series of guanidine-based hydrides were based on a five-membered mono-cyclic guanidines, whereby both N atoms of the cyclic guanidines are methylated, and the substituent of the remaining acyclic N is varied, namely unsubstituted phenyl (**2**), *p*-methoxy-phenyl (**3**), *p*-fluoro-phenyl (**4**), methyl ester (**5**) and methylated (**6**). For this series, compounds **2–6** had calculated ΔG_{H^-} in the range of 38.4–50.5 kcal mol^{-1}, which if compared to **1** is higher. Having electron withdrawing groups

Table 1 Calculated hydricity (ΔG_{H^-}, kcal mol^{-1}), CO_2 barrier ($\Delta G^{\ddagger}_{CO_2}$, kcal mol^{-1}), reaction Gibbs energy (ΔG_{rxn}, kcal mol^{-1}), relative strain ($\Delta E^{\ddagger}_{strain}$, kcal mol^{-1}), interaction ($\Delta E^{\ddagger}_{int}$, kcal mol^{-1}), activation ($\Delta E^{\ddagger}_{act}$, kcal mol^{-1}), 1st electron transfer reduction potential ($E^{\circ}_{R^+/R^\bullet}$, V *vs.* Fc^+/Fc) and reduction Gibbs energy ($\Delta G^{\circ}_{R^+/R^\bullet}$, kcal mol^{-1}) of **1–30**

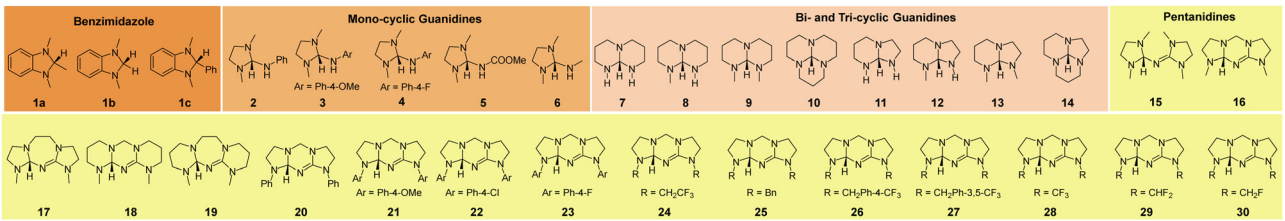

	ΔG_{H^-}	$\Delta G^{\ddagger}_{CO_2}$	ΔG_{rxn}	$\Delta E^{\ddagger}_{strain}$	$\Delta E^{\ddagger}_{int}$	$\Delta E^{\ddagger}_{act}$	$E^{\circ}_{R^+/R^\bullet}$	$\Delta G^{\circ}_{R^+/R^\bullet}$		ΔG_{H^-}	$\Delta G^{\ddagger}_{CO_2}$	ΔG_{rxn}	$\Delta E^{\ddagger}_{strain}$	$\Delta E^{\ddagger}_{int}$	$\Delta E^{\ddagger}_{act}$	$E^{\circ}_{R^+/R^\bullet}$	$\Delta G^{\circ}_{R^+/R^\bullet}$
1a	41.3	26.5	−2.4	37.2	−16.9	20.3	−2.65	61.1	**15**	22.5	22.5	−19.2	30.6	−15.3	15.3	−3.26	75.2
1b	44.4	27.1	0.3	38.3	−17.0	21.3	−2.49	57.4	**16**	27.3	23.8	−14.6	31.6	−15.2	16.4	−2.97	68.6
1c	45.6	28.5	1.3	40.1	−18.2	21.9	−2.29	52.7	**17**	26.8	23.0	−15.0	31.0	−15.3	15.7	−2.96	68.4
2	42.9	29.1	−1.0	41.8	−20.1	21.7	−2.71	62.6	**18**	26.6	22.7	−15.2	30.5	−14.3	16.2	−3.17	73.1
3	41.6	28.9	−2.2	40.4	−20.0	20.4	−3.53	81.5	**19**	18.8	21.2	−22.0	27.2	−13.6	13.6	−3.06	70.7
4	44.1	29.0	0.0	42.5	−20.4	22.0	−3.31	76.5	**20**	36.5	29.4	−6.6	40.3	−17.0	23.3	−2.57	59.4
5	50.5	30.3	5.6	43.3	−20.2	23.0	−2.36	54.4	**21**	32.8	26.6	−9.8	37.1	−16.6	20.5	−2.72	62.9
6	38.4	27.5	−5.0	41.3	−20.1	21.2	−4.23	97.5	**22**	38.7	27.0	−4.7	38.8	−18.7	20.1	−2.50	57.7
7	34.0	31.6	−8.8	39.8	−14.3	25.5	−3.18	73.4	**23**	36.0	26.3	−7.1	39.8	−17.1	22.7	−2.60	60.0
8	28.1	27.1	−13.9	34.5	−15.2	19.3	−4.24	97.8	**24**	35.6	26.0	−7.4	35.4	−16.4	19.0	−2.68	62.0
9	38.0	32.1	−5.3	40.4	−15.3	25.2	−2.95	68.1	**25**	28.1	22.9	−13.9	32.2	−15.6	16.6	−2.90	67.0
10	33.9	25.8	−8.8	32.5	−14.1	18.4	−3.08	71.0	**26**	29.8	23.6	−12.4	32.8	−15.7	17.1	−2.80	64.6
11	22.2	25.7	−19.0	34.8	−15.9	18.9	−4.47	103.2	**27**	32.7	24.3	−9.9	33.5	−16.0	17.5	−2.73	62.9
12	22.5	24.9	−18.8	33.1	−16.6	16.5	−3.57	82.5	**28**	52.1	34.4	7.0	51.5	−24.0	27.5	−2.06	47.5
13	25.4	26.6	−16.2	35.3	−16.6	18.6	−3.34	77.0	**29**	40.8	26.3	−3.3	40.5	−20.8	19.7	−2.34	54.1
14	29.0	24.1	−13.1	29.6	−13.2	16.4	−3.22	74.4	**30**	36.8	25.4	−6.4	35.1	−17.5	17.6	−2.58	59.5

in **4** and **5** are undesirable ($\Delta G^{\ddagger}_{CO_2}$ = 29.0 and 30.3 kcal mol^{-1}), while having electron donating groups such as in **3** and **6** are preferred ($\Delta G^{\ddagger}_{CO_2}$ = 28.9 and 27.5 kcal mol^{-1}), with **6** having the lowest calculated hydricity and activation barrier for CO_2 reduction. Electron donating substituent groups increases the electron density on the N, allowing hyperconjugation and weakening of the adjacent C−H bond easing H^- attack on CO_2.

Next, the second series of bicyclic and tricyclic guanidine hydrides containing only *N*-alkyl substituents were examined, starting with a symmetrical six-membered bicyclic guanidine (**7**), its mono-methylated (**8**) and dimethylated derivative (**9**), as well as unsymmetrical six- and five-membered bicyclic guanidine (**11**), its mono or bis-*N*-methylated analogues (**12** & **13**) and tricyclic guanidines (**10** & **14**). Compounds **7–14** have significantly much lower ΔG_{H^-} (22.2–34.0 kcal mol^{-1}), $\Delta G^{\ddagger}_{CO_2}$ (24.1–31.6 kcal mol^{-1}) than their monocyclic counterparts (see Table 1). Amongst the bicyclic guanidine hydrides (**7–9** & **11–13**), mono-substituted **12** most readily reduces CO_2 ($\Delta G^{\ddagger}_{CO_2}$ = 24.9 kcal mol^{-1}), whereas bis-*N*-methylated **9** the least ($\Delta G^{\ddagger}_{CO_2}$ = 32.1 kcal mol^{-1}). Activation strain model was performed to further analyse the barriers for CO_2 reduction through $\Delta E^{\ddagger}_{strain}$, $\Delta E^{\ddagger}_{interaction}$ and $\Delta E^{\ddagger}_{activation}$ (Table 1).[28] The $\Delta E^{\ddagger}_{strain}$ provides a quantitative measure for the amount of structural strain from reactants to the transition state, and $\Delta G^{\ddagger}_{CO_2}$ trend for the guanidine hydrides from **7** to **9** correlates to $\Delta E^{\ddagger}_{strain}$, where the highly strained **9** ($\Delta E^{\ddagger}_{strain}$ = 40.4 kcal mol^{-1}) has the highest $\Delta G^{\ddagger}_{CO_2}$. The rigid symmetrical tricyclic **10** (TAM) however has the lowest $\Delta G^{\ddagger}_{CO_2}$ attributed to lower $\Delta E^{\ddagger}_{strain}$ as the TS geometry is less perturbed (Table 1). The ring-fused tricyclic TAM **10** has a very symmetrical and planar guanidine moiety with low strain that allowed for the hydride to dissociate more easily (ΔG_{H^-} = 33.9). Therefore, having a planar fused-ring cyclic structure is a good molecular design strategy to lower the activation barrier for the hydride to reduce CO_2. Unsymmetrical six- five-bicyclic guanidines **11**, **12** and **13** were also calculated to have lower ΔG_{H^-} and $\Delta G^{\ddagger}_{CO_2}$ than the symmetrical ones, due to the unsymmetric guanidine hydrides being less energetically stable as their ∠NCN angles are not the ideal 120°. This inherent strain allows for their dissociation of H^- and subsequent reduction of CO_2 to be easier. Finally, the tricyclic guanidine **14** was calculated to be the best biomimetic hydride of the bi- and tri-cyclic guanidine series ($\Delta G^{\ddagger}_{CO_2}$ = 24.1 kcal mol^{-1}), affirming the importance of structure–reactivity relationship in this system. In the third series of compounds, we investigated the pentanidine series (**15–30**), which is an extended π system containing five N atoms arranged in a C_2N_5 manner. Compound **15** is structurally reminiscent of a series of previously reported chiral pentanidine catalysts.[20–22] The modelled pentanidines can be split into two subgroups, namely probing how the different pentanidine cyclic ring sizes (**15–19**) and terminal N group substituents (**20–30**) will affect ΔG_{H^-} and $\Delta G^{\ddagger}_{CO_2}$. DFT calculations revealed that the pentanidines **15–19** are by far the best reducing agents among the series, with **19** having the lowest ΔG_{H^-} (18.8 kcal mol^{-1}), and $\Delta G^{\ddagger}_{CO_2}$ (21.2 kcal mol^{-1}). This is highly encouraging as the results suggest that the pentanidine hydrides can act as excellent hydride donor for CO_2 reduction. In general, changing the tricyclic ring sizes can drastically affect planarity and ring strain of the pentanidine hydrides, which in turn affects their ΔG_{H^-} and $\Delta G^{\ddagger}_{CO_2}$. Next, the reduction potential of all the guanidinium and pentanidium were calculated to predict the ease that they can be regenerated electrochemically to reform the hydrides.

Based on the reported procedure by Musgrave, Glusac and co-workers,[14,17] the oxidised molecule can have three possible pathways for the electrochemical regeneration from the combination of proton transfer (PT) and electron transfer (ET). A detailed explanation of these pathways and calculations of pK_a and reduction potentials can be found in the ESI.† The electrochemical hydride recovery process follows the ET → PT → ET (e^- + H^+ + e^- or eHe for short) reduction pathway (see ESI† Scheme S2 and Table S1), so the barrier associated with the reduction process is primarily determined by the first ET step, which is $E^{\circ}_{R^+/R\bullet}$ or its equivalent $\Delta G^{\circ}_{R^+/R\bullet}$ as summarized in Table 1. The calculated pK_a (PT) and second ET complete data for all molecules are available in the ESI† Table S2. It is also noted that based on the result of the tricyclic pentanidine (**15–19**), further screening by substituting the *N*-methyl groups on **16** (**20–30**) were carried out as it has a low $\Delta G^{\ddagger}_{CO_2}$ and less negative $E^{\circ}_{R^+/R\bullet}$. The pentanidium of **22**, **29** and **30** have more positive reduction potentials (−2.50, −2.34, −2.58 V, respectively) and would be more easily reduced. These pentanidines are expected to more easily regenerated electrochemically to participate in the next catalytic cycle.

To better understand the guanidine/pentanidine overall redox reactivity, Fig. 1a was plotted to understand the relationship between CO_2 reduction ($\Delta G^{\ddagger}_{CO_2}$) and their ease to regenerate electrochemically ($\Delta G^{\circ}_{R^+/R\bullet}$). Fig. 1b depicts the exothermic hydride transfer (−6.4 kcal mol^{-1}) from **30** to a molecule of CO_2 *via* transition state **TS30** with an activation barrier of 25.4 kcal mol^{-1}, to form the pentanidinium cation **30_ox** and a formate anion. The quadrants in Fig. 1a are marked according to the maximum $\Delta G^{\circ}_{R^+/R\bullet}$ and $\Delta G^{\ddagger}_{CO_2}$ values of the benzimidazoles (**1a**, **1b** and **1c**). Ideally, the best organohydrides would fall into quadrant I, *i.e.*, low $\Delta G^{\circ}_{R^+/R\bullet}$ (easier to regenerate the hydride) and low $\Delta G^{\ddagger}_{CO_2}$ (easier CO_2 reduction) values. The mono-cyclic guanidine hydrides **2–6** have similar CO_2 reduction performance (quadrants II and III), while bi- and tri-cyclic guanidine hydrides **7–14** are better reducing agents for CO_2, *i.e.*, further left of quadrant II. For **2–14**, they are not ideal being reduced from guanidinium back to guanidine hydride. The pentanidine group **15–19** all fall within quadrant II, suggesting that they are by far excellent for CO_2 reduction but not ideal when are reduced from pentanidium to pentanidine hydride. However, installing electron-withdrawing Cl, F, CHF_2 or CH_2F on **16** amine group, made pentanidium **22**, **23**, **29**, and **30** better oxidants and their corresponding pentanidine hydrides more

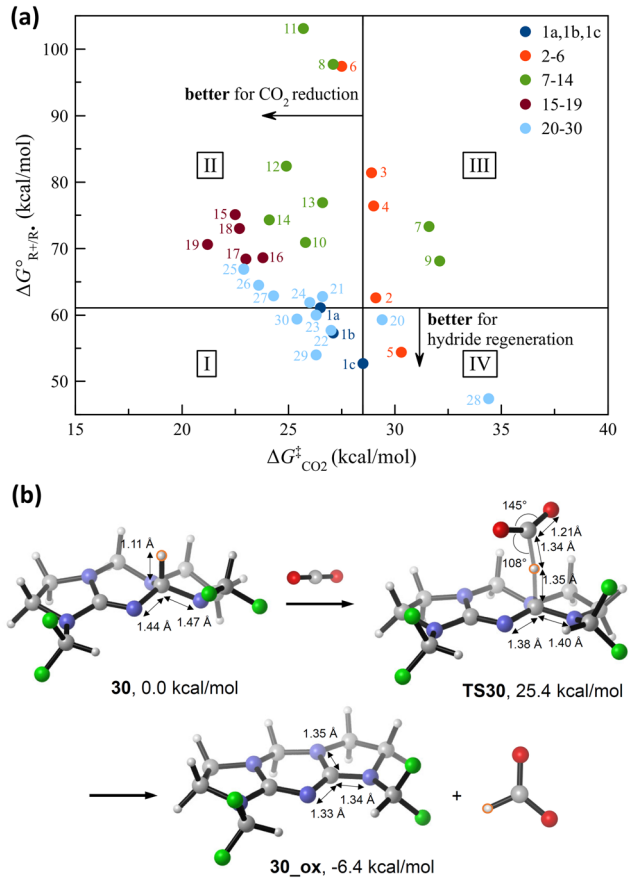

Fig. 1 (a) CO_2 reduction $\Delta G^{\ddagger}_{CO_2}$ and redox $\Delta G^{\circ}_{R+/R\bullet}$ for **1–30**. The quadrants are divided based on maximum of the benzimidazoles (**1a**, **1b** and **1c**); (b) representative 3-D rendered optimized structures of **30**, **TS30** and **30_ox** with key bond length (Å), angles (°) and relative Gibbs energy. Atoms are color-coded: gray (carbon), white (hydrogen) and highlighted (hydride), blue (nitrogen), and green (fluorine).

capable as reducing agents for CO_2 albeit having slightly higher $\Delta G^{\ddagger}_{CO_2}$ (quadrant I). Indeed, having electron-withdrawing groups stabilize the organohydride, allowing it to be more easily recovered from its oxidised state, but at the same time penalizes its hydride donating abilities. Fine-tuning of the electronics of the hydrides is needed to achieve an optimal redox balance.

In conclusion, our computational calculations suggest that the guanidine-based organohydrides can be excellent hydride donors and further DFT analysis for the mono-, bi- and tri-cyclic guanidines, and tricyclic pentanidines series revealed that balancing the CO_2 reducing ability of the guanidine/pentanidine and oxidizing ability of the guanidinium/pentanidium needs to be achieved. This work serves to guide the robust molecular design of efficient biomimetic guanidine/pentanidine organohydrides and the results will be critical to guide experiment to synthesize promising electrochemically regenerative organohydrides for CO_2 reduction.

This work is supported by the Australian Research Council (DE210100053, R. L.) and University of Wollongong (RITA grant, H. Y. and R. L.; VC fellowship, R. L.). Computational resources were generously provided by the National Computational Infrastructure through the NCMAS and UOW-NCI schemes.

Conflicts of interest

There are no conflicts to declare.

Notes and references

1 O. S. Bushuyev, P. De Luna, C. T. Dinh, L. Tao, G. Saur, J. van de Lagemaat, S. O. Kelley and E. H. Sargent, *Joule*, 2018, **2**, 825.
2 E. Graf and W. Leitner, *J. Chem. Soc., Chem. Commun.*, 1992, 623.
3 S. Chatterjee, I. Dutta, Y. Lum, Z. Lai and K.-W. Huang, *Energy Environ. Sci.*, 2021, **14**, 1194.
4 E. S. Wiedner, M. B. Chambers, C. L. Pitman, R. M. Bullock, A. J. Miller and A. M. Appel, *Chem. Rev.*, 2016, **116**, 8655.
5 S. Ilic, A. Alherz, C. B. Musgrave and K. D. Glusac, *Chem. Soc. Rev.*, 2018, **47**, 2809.
6 R. B. Gordon, M. Bertram and T. E. Graedel, *Proc. Natl. Acad. Sci. U. S. A.*, 2006, **103**, 1209.
7 Y. Feng, W. An, Z. Wang, Y. Wang, Y. Men and Y. Du, *ACS Sustainable Chem. Eng.*, 2020, **8**, 210.
8 S. Zhang, Q. Fan, R. Xia and T. Meyer, *Acc. Chem. Res.*, 2020, **53**, 255.
9 S. Ilic, J. L. Gesiorski, R. B. Weerasooriya and K. D. Glusac, *Acc. Chem. Res.*, 2022, **55**, 844.
10 C. Zheng and S.-L. You, *Chem. Soc. Rev.*, 2012, **41**, 2498.
11 A. Hantzsch, *Ber. Dtsch. Chem. Ges.*, 1881, **14**, 1637.
12 Q.-A. Chen, M.-W. Chen, C.-B. Yu, L. Shi, D.-S. Wang, Y. Yang and Y.-G. Zhou, *J. Am. Chem. Soc.*, 2011, **133**, 16432.
13 D. R. Weinberg, C. J. Gagliardi, J. F. Hull, C. F. Murphy, C. A. Kent, B. C. Westlake, A. Paul, D. H. Ess, D. G. McCafferty and T. J. Meyer, *Chem. Rev.*, 2012, **112**, 4016.
14 S. Ilic, A. Alherz, C. B. Musgrave and K. D. Glusac, *Chem. Commun.*, 2019, **55**, 5583.
15 X. Yang, J. Walpita, D. Zhou, H. L. Luk, S. Vyas, R. S. Khnayzer, S. C. Tiwari, K. Diri, C. M. Hadad, F. N. Castellano, A. I. Krylov and K. D. Glusac, *J. Phys. Chem. B*, 2013, **49**, 15290.
16 C.-H. Lim, S. Ilic, A. Alherz, B. T. Worrell, S. M. Bacon, J. T. Hynes, K. D. Glusac and C. B. Musgrave, *J. Am. Chem. Soc.*, 2019, **141**, 272.
17 M. F. Alkhater, A. W. Alherz and C. B. Musgrave, *Phys. Chem. Chem. Phys.*, 2021, **23**, 17794.
18 B. D. Ostojić, B. Stanković, D. S. Đorđević and P. Schwerdtfeger, *Phys. Chem. Chem. Phys.*, 2022, **24**, 20357.
19 W. Yang, D. Tan, R. Lee, L. Li, Y. Pan, K.-W. Huang, C.-H. Tan and Z. Jiang, *Chem. – Asian J.*, 2012, **7**, 771.
20 X. Zhang, J. Ren, S. M. Tan, D. Tan, R. Lee and C.-H. Tan, *Science*, 2019, **363**, 40.
21 W. Cao, D. Tan, R. Lee and C.-H. Tan, *J. Am. Chem. Soc.*, 2018, **140**, 1952.
22 R. Lee, C. B. E. Chao, X. Ban, S. M. Tan, H. Yu, C. J. T. Hyland and C.-H. Tan, *J. Org. Chem.*, 2022, **87**, 4029.
23 C. D. N. Gomes, E. Blondiaux, P. Thuéry and T. Cantat, *Chem. – Eur. J.*, 2014, **23**, 7098.
24 C. Villiers, J.-P. Dognon, R. Pollet, P. Thuéry and M. Ephritikhine, *Angew. Chem., Int. Ed.*, 2010, **49**, 3465.
25 C.-Y. Yang, Y.-F. Ding, D. Huang, J. Wang, Z.-F. Yao, C.-X. Huang, Y. Lu, H.-L. Un, F.-D. Zhuang, J.-H. Dou, C.-A. Di, D. Zhu, J.-Y. Wang, T. Lei and J. Pei, *Nat. Commun.*, 2020, **11**, 3292.
26 E. H. Wong, G. R. Weisman, D. C. Hill, D. P. Reed, M. E. Rogers, J. S. Condon, M. A. Fagan, J. C. Calabrese, K.-C. Lam, I. A. Guzei and A. L. Reingold, *J. Am. Chem. Soc.*, 2000, **122**, 10561.
27 I. V. Alabugin and T. A. Zeidan, *J. Am. Chem. Soc.*, 2002, **124**, 3175.
28 W.-J. van Zeist and F. M. Bickelhaupt, *Org. Biomol. Chem.*, 2010, **8**, 3118.

